BJUI
BJU International

Lesion volume predicts prostate cancer risk and aggressiveness: validation of its value alone and matched with prostate imaging reporting and data system score

Eugenio Martorana*, Giacomo Maria Pirola*, Michele Scialpi†, Salvatore Micali*, Andrea Iseppi*, Luca Reggiani Bonetti‡, Shaniko Kaleci§, Pietro Torricelli¶ and Giampaolo Bianchi*

*Department of Urology, University of Modena and Reggio Emilia, Modena, †Department of Surgical and Biomedical Sciences, Division of Radiology 2, Perugia University, Perugia , ‡Departments of Diagnostic Medicine and Public Health -Section of Pathology, §Medical Statistic, and ¶Diagnostic Imaging, University of Modena and Reggio Emilia, Modena, Italy

Objective

To demonstrate the association between magnetic resonance imaging (MRI) estimated lesion volume (LV), prostate cancer detection and tumour clinical significance, evaluating this variable alone and matched with Prostate Imaging Reporting and Data System version 2 (PI-RADS v2) score.

Patients and methods

We retrospectively analysed 157 consecutive patients, with at least one prior negative systematic prostatic biopsy, who underwent transperineal prostate MRI/ultrasonography fusion-targeted biopsy between January 2014 and February 2016. Suspicious lesions were delineated using a 'region of interest' and the system calculated prostate volume and LV. Patients were divided in groups considering LV (≤0.5, 0.5–1, ≥1 mL) and PI-RADS score (1–5). We considered clinically significant prostate cancer as all cancers with a Gleason score of ≥3 + 4 as suggested by PI-RADS v2. A direct comparison between MRI estimated LV (MRI LV) and histological tumour volume (HTV) was done in 23 patients who underwent radical prostatectomy during the study period. Differences between MRI LV and HTV were assessed using the paired sample *t*-test. MRI LV and HTV concordance was verified using a Bland–Altman plot. The chi-squared test and logistic and ordinal regression models were used to evaluate difference in frequencies.

Results

The MRI LV and PI-RADS score were associated both with prostate cancer detection (both $P < 0.001$) and with significant prostate cancer detection ($P < 0.001$ and $P = 0.008$, respectively). When the two variables were matched, increasing LV increased the risk within each PI-RADS group. Prostate cancer detection was 1.4-times higher for LVs of 0.5–1 mL and 1.8-times higher for LVs of ≥1 mL; significant prostate cancer detection was 2.6-times for LVs of 0.5–1 mL and 4-times for LVs of ≥1 mL. There was a positive correlation between MRI LV and HTV ($r = 0.9876$, $P < 0.001$). Finally, Bland–Altman analysis showed that MRI LV was underestimated by 4.2% compared to HTV. Study limitations include its monocentric and retrospective design and the limited cohort.

Conclusions

This study demonstrates that PI-RADS score and the MRI LV, independently and in combination, are associated with prostate cancer detection and with tumour clinical significance.

Keywords

PI-RADS v2 score, lesion volume, prostate cancer detection, clinically significant prostate cancer, tumour aggressiveness

Introduction

Currently, mpMRI represents the most sensitive imaging method for prostate cancer detection [1–3], capable of giving a precise localisation of suspicious areas within the prostate and guiding clinical decision-making for suspected prostate cancer [4].

The European Society of Urogenital Radiology drafted guidelines, including a scoring system, to characterise prostate

 | doi:10.1111/bju.13649
Published by John Wiley & Sons Ltd. www.bjui.org

mpMRI suspicious lesions known as PI-RADS™, recently updated to PI-RADS™ version 2 (v2), to help clinicians in the interpretation and reporting of these findings [5,6]. Published data seems to validate this scoring system, with the advantage of increasing the detection of aggressive tumours (Gleason score ≥7) and reducing the detection of indolent prostate cancers (Gleason score ≤6 and volume <0.5 mL) compared with random ultrasonography (US)-guided biopsies [7].

PI-RADS v2 introduced a tumour size criterion compared to the first version. Based on this parameter, a lesion with a PI-RADS score of 4 is upgraded to the higher score when its diameter is >15 mm [8]. However, prostate cancer is a solid tumour and has a defined three dimensional shape, so its characteristics are better represented by a volume than a scanned surface.

There is a lack of studies evaluating the role of mpMRI pre-biopsy lesion volume (LV) and its relation to cancer diagnosis and its characteristics.

The aim of the present study was to investigate the association between suspicious lesion (SL) volume, prostate cancer detection and tumour clinical significance by evaluating this variable alone and in combination with PI-RADS v2 score.

Patients and methods

Between January 2014 and February 2016, using prostatic mpMRI, we retrospectively evaluated, in the Urology Department of University of Modena and Reggio Emilia (Italy), a cohort of patients with persistent high clinical suspicion of prostate cancer [i.e. persistent elevation of PSA level, suspicious DRE, previous diagnosis of atypical small acinar proliferation (ASAP) or multifocal high-grade prostatic intraepithelial neoplasia (HGPIN), and a combination thereof].

All patients had undergone at least one previous prostate mapping. Specifically, 87 patients (55.4%) had undergone one previous prostate mapping, 41 (26,1%) had undergone two and 29 (18.5%) had undergone three previous prostate mappings. According to the diagnosis at the previous prostatic mapping: 34 patients (21.7%) had ASAP; 51 (32.5%) had HGPIN, and 72 (45.8%) had BPH/inflammation.

The study included 157 patients in which at least one SL or index lesion was detected. These patients were enrolled for transperineal MRI/US fusion-targeted biopsy (FTBx) using the BiopSee® system (MedCom GmbH, Darmstadt, Germany) [9]. All detected SLs were classified according to the PI-RADSv2 score.

We performed the FTBx in all patients with at least one SL with a PI-RADS score of ≥2. All patients with only one SL and a PI-RADS score of 2 were informed of their low risk of a cancer diagnosis but they agreed to undertake the procedure. Patients with lesions with PI-RADS scores of 1 were enrolled only if at least one coexistent lesion was detected with a PI-RADS score of ≥2.

The median (SD, range) age was 65.02 (6.8, 47–79) years, the PSA level was 10.7 (11.29, 1.0–75.0) ng/mL, and prostate volume was 70.4 (33.73, 21–196) mL. Written informed consent was obtained from all patients and a waiver of informed consent was issued to each patient. An anonymous excel file was created giving a progressive number to each patient.

To standardise the reporting of our data we followed the main statements of the Standards of reporting for MRI-targeted biopsy studies (START) guidelines [10]. Table 1 (START table) summarises the patients' characteristics and a detailed study flowchart is shown in Fig. 1.

Accordant with PI-RADS v2 criteria [6], outcome measures were reported as follows: a) any prostate cancer, to evaluate the relationship between PI-RADS score, LV and

Table 1 START table showing pre-biopsy characteristics (n = 157), mpMRI findings, biopsy details, and RALP outcomes (n = 23).

Variable	Value
Men included in analysis, *n*	157
Age, years, median (IQR)	65 (47–79)
Pre-biopsy PSA level, ng/ml, median (IQR)	10.7 (1–75.0)
Suspicious DRE findings (≥T2), *n* (%)	12 (8)
Prostate volume, mL, median (IQR)	70.40 (21.00–196.56)
PSA density, ng/mL/mL, median (IQR)	0.18 (0.04–1.32)
Patients with prior prostate biopsy, *n* (%)	157 (100)
Patients without prior biopsy, *n*	0
Patients with 1 prior biopsy	87
Patients with 2 prior biopsy	41
Patients with 3 prior biopsy	29
Number of cores in prior biopsy, *n*, median (IQR)	17 (12–36)
Patients undergoing active surveillance, *n*	0
Days from mpMRI to biopsy, median (IQR)	52 (30–78)
Days from mpMRI to radical prostatectomy, median (IQR)	74 (50–90)
Men with PI-RADS ≥2 lesions on mpMRI, *n* (%)	157 (100)
Number of lesions PI-RADS ≥2	277 (98)
Patients with one PI-RADS ≥2 lesion	74
Patients with two PI-RADS ≥2 lesions	51
Patients with three or more PI-RADS ≥2 lesions	32
Overall PI-RADS score 2 lesions, *n* (% of PI-RADS ≥2)	108 (39)
Overall PI-RADS score 3 lesions, *n* (% of PI-RADS ≥2)	75 (27)
Overall PI-RADS score 4 lesions, *n* (% of PI-RADS ≥2)	66 (24)
Overall PI-RADS score 5 lesions, *n* (% of PI-RADS ≥2)	28 (10)
Biopsies per patient, median (IQR)	28 (26–34)
Systematic biopsies per patient, median (IQR)	24 (24–24)
FTBx per patient and per lesion, median (IQR)	4 (2–10), 2.5 (1–5)
Overall lesions in radical prostatectomy specimen, *n*	32
Index tumour lesions, *n*	23
Additional lesions, *n*	9
Patients with additional lesions, *n* (%)	5 (22)

IQR, interquartile range.

Fig. 1 Study flow chart.

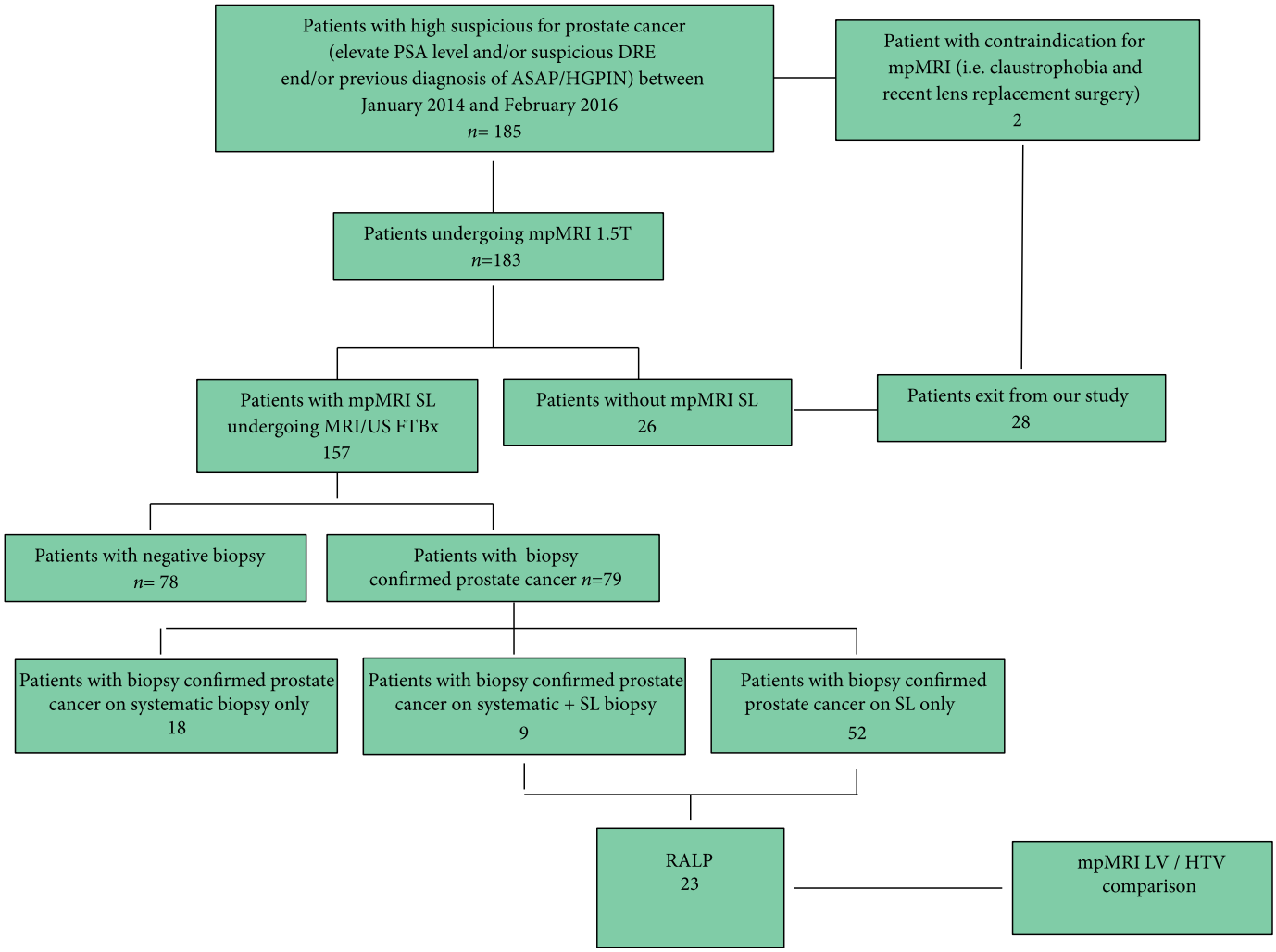

prostate cancer detection rate; b) significant prostate cancer (Gleason score ≥3 + 4, or pathologically determined tumour volume >0.5 mL, or pathologically determined extra-prostatic extension) to evaluate the relationship between PI-RADS score, LV and significant prostate cancer detection.

After prostate cancer diagnosis, data regarding final pathological specimens of patients who underwent robot-assisted laparoscopic radical prostatectomy (RALP) during the study period were collected. Histological tumour volume (HTV) and MRI LV were compared to verify a correlation between the two measurements.

Finally, early complications such as acute urinary retention and perineal haematoma were recorded before hospital discharge. Moreover, all patients were followed-up at 20 days after FTBx to collect data on procedure-related late complications, e.g. fever, haematuria, acute urinary retention, perineal haematoma, haemospermia.

Prostatic mpMRI parameters

All mpMRI in this study were performed using a 1.5-Tesla Achieva MRI machine (Philips Healthcare, Best, The Netherlands) with an endorectal (Endorectal MRI-probe, Medrad Performance for Life eCoil) and superficial SENSE cardiac phased-array coil with five channels (Cardiac Synergy Coil, Philiphs Medical Systems, Detroit, MI, USA).

The protocol for prostate MRI included: axial T1-weighted fast spin-echo (FSE) imaging; axial, sagittal and coronal T2-weighted (T2W) FSE imaging; axial diffusion-weighted imaging (DWI; b values of b 0, 350, 700, 1000 s/mm^2) with apparent diffusion coefficient (ADC) map reconstructions; and axial T1-weighted fat-suppression dynamic contrast-enhanced (DCE)-MRI. T2W image slice thickness and acquisition resolution were 3 mm and 0.5 × 0.5 mm, respectively. DCE temporal resolution was 15 s for 3 min (six phases) without breath-holding, following an i.v. single dose of 0.2 mL/kg at 2.5 mL/s of gadopentetate dimeglumine (Magnevist; Bayer

Schering Pharma AG, Berlin, Germany). Only a qualitative analysis for DWI and DCE-MRI was carried out.

Two radiologists, with 4 years of experience in the field of prostate MRI (P.T. and M.S.), evaluated the mpMRI, searching for the presence of any suspicious area and reaching a consensus. The index lesion was defined as the largest SL on axial T2W imaging and/or DWI/ADC. The axial scan of the DWI/ADC slice containing the greatest suspect area of the index lesion was considered for location matching analysis, and denoted as the apex, middle, or base of the prostate for analyses of three equal trisections of the prostate. Specifically, the centre of the index lesion was defined as the point of intersection of the higher lesion height and width using the lowest ADC value. Finally, the location of the index tumour was recorded according to the 39 PI-RADS sectors.

LV calculation

A preliminary study on T2W images, on which the boundaries of the prostate and SL were traced, was done in all patients using the BiopSee system.

Considering that the dominant sequence for a SL in the peripheral zone is the DWI/ADC, the peripheral SL is firstly detected on axial DWI/ADC sequence and after on the corresponding axial T2W imaging. Secondly, axial DWI/ADC and T2W imaging sequences are imported on the BiopSee system. Then, the axial DWI/ADC sequences are overlapped on the corresponding T2W images to detect the SL on the BiopSee system. Finally, the radiologist manually traces the SL contours only on axial T2W sequences before the MRI/US fusion is done.

Specifically, the boundaries of the SLs are rigorously delineated on the axial plane, using a 'region of interest' (ROI) one scan after the other until the entire SL is marked. Each border is automatically and real-time reproduced also on the sagittal and coronal planes by the system obtaining a 'volume of interest' (VOI). The volumes of all contoured VOI are automatically calculated. The calculation uses a three-dimensional (3D) derivation of Gauss's Theorem algorithm and gives the exact result of the volume enclosed by the triangulated surface of a VOI. The use of the Gauss's Theorem algorithm implies that the intersecting parts are counted for each involved VOI [11–13]. The calculated volumes, expressed in millilitres, are displayed in the text field in the upper left corner of the 3D-model view. Finally, a graphic 3D representation of the SL within the prostate is constructed (Fig. 2)

Fig. 2 Suspicious lesion (SL) affecting the left peripheral zone of the prostate. Boundaries of the SL are rigorously delineated in the axial plane (**C**), using a region of interest (ROI) one scan after the other until the entire SL is marked. Each border is automatically and real-time reproduced also in the sagittal (**B**) and coronal (**A**) planes by the system obtaining a volume of interest (VOI). The system automatically calculates both the prostate and SL volumes giving a value in millilitres (mL) (**D**).

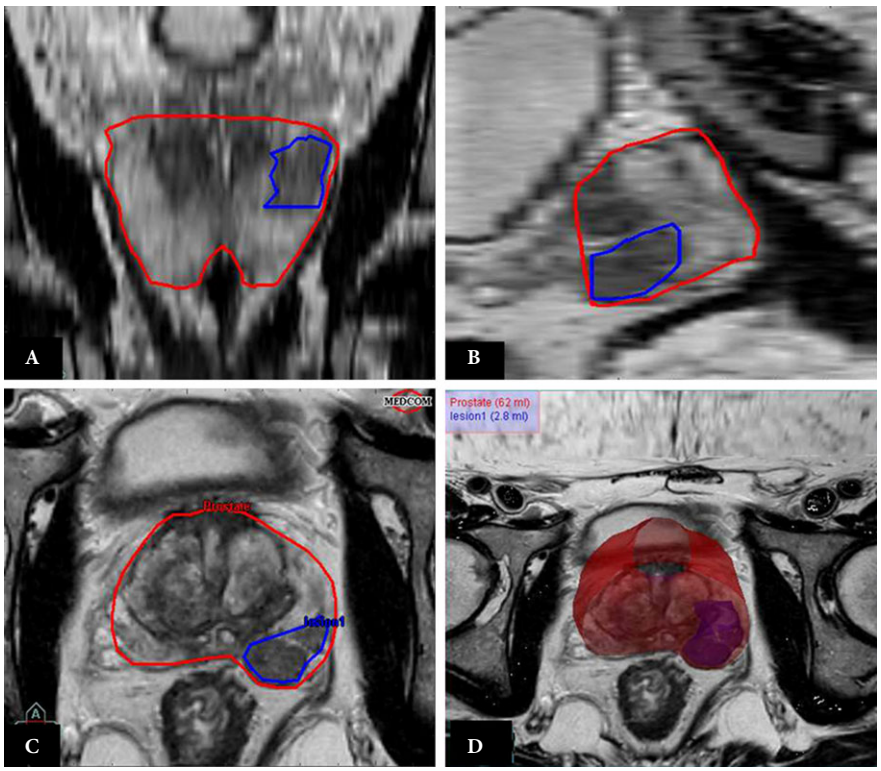

Pathological analyses of RALP specimens and HTV measurement

After RALP, the surgical specimens were fixed in 10% buffered neutral formalin. The prostate surface was inked before the dissection. The prostate was sectioned in to three equal trisections: apex, middle, and base. Then, routine haematoxylin and eosin stained serial 3-µm thick sections were taken from each trisection. The index tumour was defined as the largest tumour focus taking into account Gleason score.

The HTV measurement was obtained for the index tumour as follow. The tumour length maximum diameter was defined as the largest tumour dimension on any cross-section. Tumour width was considered as the maximal width perpendicular to the tumour length maximum diameter. The tumour thickness was calculated as the number of slices containing index tumour multiplied by the average slice thickness of the respective specimen. All measures were performed without a correction factor as described by Baco et al. [14]. According to Perera et al. [15], the HTV was calculated using the ellipsoid volume formula using the longest perpendicular diameters: depth × width × length × 0.523.

Figure 3 shows the comparison between the radiological SL in the axial plane and the appearance of the corresponding pathologically confirmed tumour.

The pathology slide with the greatest cross-section of the index tumour was used for location matching analysis. The centre of the index tumour was defined as the point of intersection of the lesion height and width dimensions, and the location of the index tumour was recorded according to the 39 PI-RADS sectors.

Biopsy technique

The BiopSee is a system designed to take FTBx. All FTBx were performed by a single experienced urologist (E.M.) under general anaesthesia to ensure patient immobility. Even when anaesthesia is not the standard practice, FTBx is a highly accurate procedure. Thus, all small patient movements (i.e. voluntary movements of the chest, cough, sneezing, speech, etc.) are inevitably reflected on the pelvis and can jeopardise the goodness of fusion, once it has been done, affecting the benefits of the procedure.

US of the prostate was performed in a cranio-caudal direction in order to acquire the entire axial 2D prostate volume. Biopsee then reworked these sequences to provide a 3D US reconstruction of the gland on which to perform US/MRI images fusion with T2W sequences previously imported and delineated (Fig. 4). FTBx was performed on any SL followed by a further 24 random samples using the Ginsburg Study Group scheme [16]. The needle, inserted through the transperineal template, passes through the prostate along a longitudinal trajectory until the target area is reached. Samples were obtained with an 18 G × 16 cm disposable biopsy needle, mounted on a reusable biopsy gun (Pro-Mag Ultra®, Angiotech, Stenløse, Denmark; Fig. 5). All samples were collected in blocks, named according to the sampling area, and sent separately for histopathological examination. After each biopsy, the exact 3D pickup location was recorded and stored by the software.

Statistical analysis

Data were analysed by statistical package STATA13 (StataCorp. 2011. Stata: Release 12 Statistical Software, College Station, TX, USA: StataCorp LP). Differences between MRI LV and HTV were assessed using the paired sample *t*-test. MRI LV and HTV concordance was verified using a Bland–Altman plot. The chi-squared test and logistic and ordinal regression models were used to evaluate differences in frequencies. Continuous variables are expressed as means [standard deviations (SDs)] and range. The selected level of statistical significance was $P \leq 0.05$.

Fig. 3 Comparison between MRI SL and pathological confirmed tumour. (**A**) Contouring of the MRI SL in axial plane by BiopSee Sistem®. (**B**) Contouring of the pathological confirmed tumour in the corresponding slide (slices were stained with haematoxylin-eosin after being embedded in paraffin).

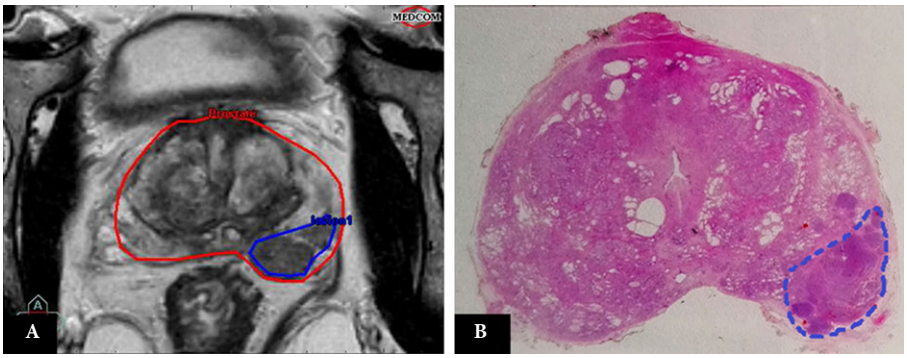

Fig. 4 Suspicious lesion affecting the anterior zone of the prostate. In this figure, MRI/US fusion was performed and the obtained MRI VOI was overlapped to the equivalent US scan. Histopathological examination revealed a Gleason score 7 (3 + 4) prostate cancer in all targeted cores.

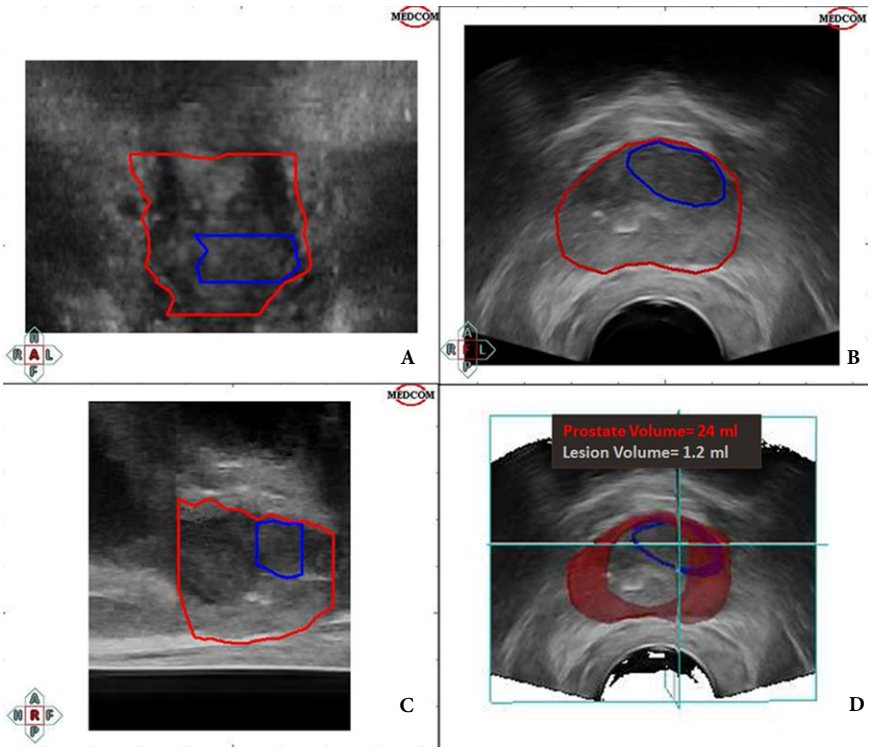

Fig. 5 PRO-MAG® ultra. This an automatic and reusable biopsy gun for histological core biopsies: (**A**) Needle allocation system; (**B**) Biopsy gun ready for use; (**C**) The needle has an echogenic tip for accurate placement under US guidance; (**D**) Biopsy core.

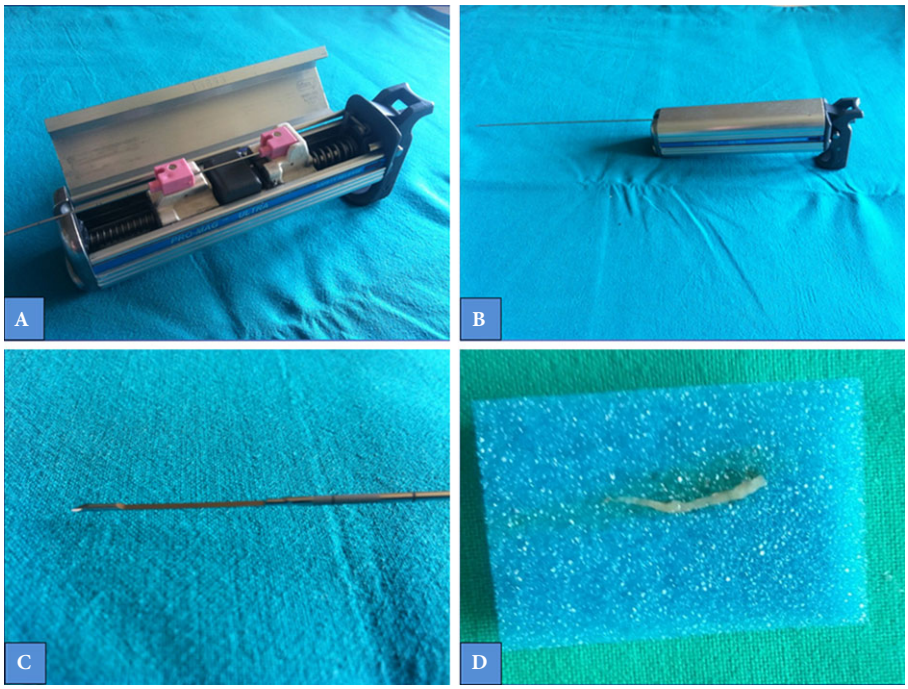

Results

The overall detection rate was 50.32% (79/157 patients): 52 patients (65.83%) had prostate cancer detected on FTBx only, 18 (22.78%) on systematic biopsy only (total number of positive random core in these patients was 38), and nine (11.39%) on both FTBx and systematic biopsy ($P < 0.001$). All the significant prostate cancers were detected by FTBx. Table 2 show the Gleason score distribution considering both targeted and random biopsies.

In all, 283 SLs were detected (range 1–4, median 1.83). The median (SD, range) LV was 0.67 (1.18, 0.02–12) mL. According to LV, the SLs were divided in three groups: 168 with a LV of ≤0.5 mL, 71 between 0.5 and 1 mL, and 44 ≥ 1 mL. Moreover, six SLs were classified as PI-RADS 1, 108 as PI-RADS 2, 75 as PI-RADS 3, 66 as PI-RADS 4, and 28 as PI-RADS 5.

Histologically, prostate cancer was confirmed in 74/283 (26.15%) SLs. Table 3 summarises the SL characteristics matching their PI-RADS score and LV and considering the histological result as positive or negative. Figure 6 shows the LV distribution according to the histological results.

The prostate cancer detection rate increased with increasing PI-RADS score, rising from 0% to 2.8% (three of 108), to 12% (nine of 75), to 57.6% (38/66) and to 85.7% (24/28) for PI-RADS score 1, 2, 3, 4 and 5, respectively ($P < 0.001$). Using a univariate logistic regression model and considering PI-RADS score 1 plus PI-RADS score 2 as the comparison group, we found that prostate cancer diagnosis was 5-times higher for PI-RADS 3, 50-times higher for PI-RADS 4, and 222-times higher for PI-RADS 5 lesions.

Prostate cancer diagnosis also increased with increasing LV from 17.3% (29/168) to 35.2% (25/71) to 45.5% (20/44) when the LV was ≤0.5, 0.5–1, and ≥1 mL, respectively ($P < 0.001$). Using a univariate logistic regression model and considering a LV of 0.5 mL as the comparison group, we found that prostate cancer risk was 2.6-times higher for LVs between 0.5 and 1 mL and 4-times higher for LVs of >1 mL. Finally, using an ordinal logistic regression model and considering a LV of <0.5 mL as the comparison group, we found that, within each PI-RADS score group, the probability of finding a prostate cancer was 1.4-times higher when the LV was between 0.5 and 1 mL and 1.8-times higher when the LV was ≥1 mL.

Table 4 shows prostate cancer-confirmed lesions and reports the relationship between the LV and the biopsy Gleason score. Significant prostate cancer was detected in 25/74 (33.8%) compared to 49/74 (66.2%) SLs in which the Gleason score was ≤6 ($P = 0.022$). Considering LV, the significant

Table 2 Gleason score distribution considering both targeted (horizontally) and random biopsies (vertically).

	Gleason score	Random, *n*						Total, *n*
		Negative	Gleason score 6 (3 + 3)	Gleason score 7 (3 + 4)	Gleason score 7 (4 + 3)	Gleason score 8 (4 + 4)	Gleason score 8 (5 + 3)	
Targeted	Negative	78	18	0	0	0	0	96
	6 (3 + 3)	29	9	0	0	0	0	38
	7 (3 + 4)	11	0	0	0	0	0	11
	7 (4 + 3)	5	0	0	0	0	0	5
	8 (4 + 4)	5	0	0	0	0	0	5
	8 (5 + 3)	2	0	0	0	0	0	2
Total, *n*		130	27	0	0	0	0	157

Table 3 PiVo table showing SL characteristics matching their PI-RADS score, LV and histological results (positive or negative).

LV, mL	Positive, *n*					Subtotal, *n*	Negative, *n*					Subtotal, *n*	Total, *n*	P
	PI-RADS v2 score						PI-RADS v2 score							
	1	2	3	4	5		1	2	3	4	5			
≤0.5	0	3	5	17	4	29	6	74	43	15	1	139	168	PI-RADS score < 0.001
0.5–1	0	0	1	15	9	25	0	22	12	11	1	46	71	LV < 0.001
≥1	0	0	3	6	11	20	0	9	11	2	2	24	44	
Total, *n*	0	3	9	38	24	74	6	105	66	28	4	209	283	

With this table is possible understand the additional value of LV when the two variables are matched. For example, in our study the prostate cancer detection rate for the SLs group with PI-RADS score 3 and volume between 0.5 and 1 mL was [1 (positive lesion)/1 (positive lesion) + 12 (negative lesions) = 7.7%]. The prostate cancer detection rate was significantly higher for SLs group with the same PI-RADS score and a LV of >1 mL [3 (positive lesion) /3 (positive lesion) + 11 (negative lesion) = 21.4%].

Fig. 6 Box plot representation of LV distribution according to positive or negative histological results. For negative SL volumes the median value was 0.37 mL, for positive SL volumes the median value was 0.59 mL.

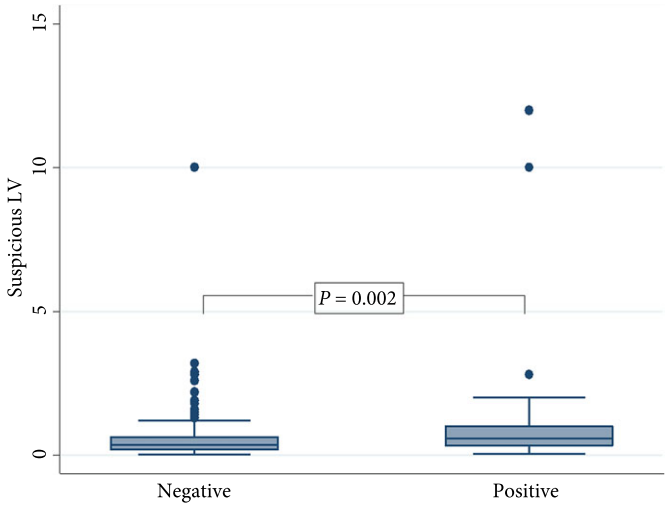

prostate cancer detection rate was as follows (Table 4): four of 29 tumours (13.8%) with a LV of ≤0.5 mL, 10/25 (40%) with a LV of 0.5–1 mL, and 11/20 tumours (55%) with a LV of ≥1 mL (P = 0.008). Figure 7 shows the LV distribution according to Gleason score.

Considering the PI-RADS score, the significant prostate cancer detection rate was as follows (Table 5): none with PI-RADS score 1, none of six with PI-RADS score 2, one of nine with PI-RADS score 3, 11/38 (28.9%) with PI-RADS score 4, 13/24 (54.2%) with PI-RADS score 5 (P = 0.03). Moreover, Table 6 shows the association between significant prostate cancer diagnosis and the two variables (i.e. PI-RADS score and LV) when matched. Using an ordinal logistic regression model and considering a LV of ≤0.5 mL as the comparison group, we found that, within each PI-RADS lesions group, the probability of detecting a higher Gleason score (≥7) is 3.5-times more when the LV was between 0.5 and 1 mL, and 4.3-times more when the LV was ≥1 mL. Moreover, Table 6 allows identification of significant prostate cancer detection rate based on each PI-RADS score and LV group. In fact, considering the SL group with a LV of ≤0.5 mL, the significant prostate cancer detection rate was 0% for SLs with PI-RADS scores of 1, 2 and 3; it increased to three of 32 (9.4%) for SLs with a PI-RADS score of 4 and was one in five for SLs with a PI-RADS score of 5 (P = 0.002). For the SL group with a LV between 0.5 and 1 mL, significant prostate

Table 4 VoGle table showing positive SLs grouped considering LV and Gleason score. Aggressive tumour rate (Gleason score ≥7) increased with increasing LV.

LV, mL	Positive Gleason score, *n*					Total, *n*	*P*
	6 (3 + 3)	7 (3 + 4)	7 (4 + 3)	8 (4 + 4)	8 (5 + 3)		
≤0.5	25	2	2	0	0	29	0.008
0.5–1	15	6	1	3	0	25	
≥1	9	3	2	4	2	20	
Total, *n*	49	11	5	7	2	74	

Fig. 7 Box plot representation of LV distribution according to Gleason score. (**A**) LV distribution considering non-aggressive (Gleason score ≤6) and aggressive (Gleason score ≥7) tumours. (**B**) LV distribution inside each Gleason score group.

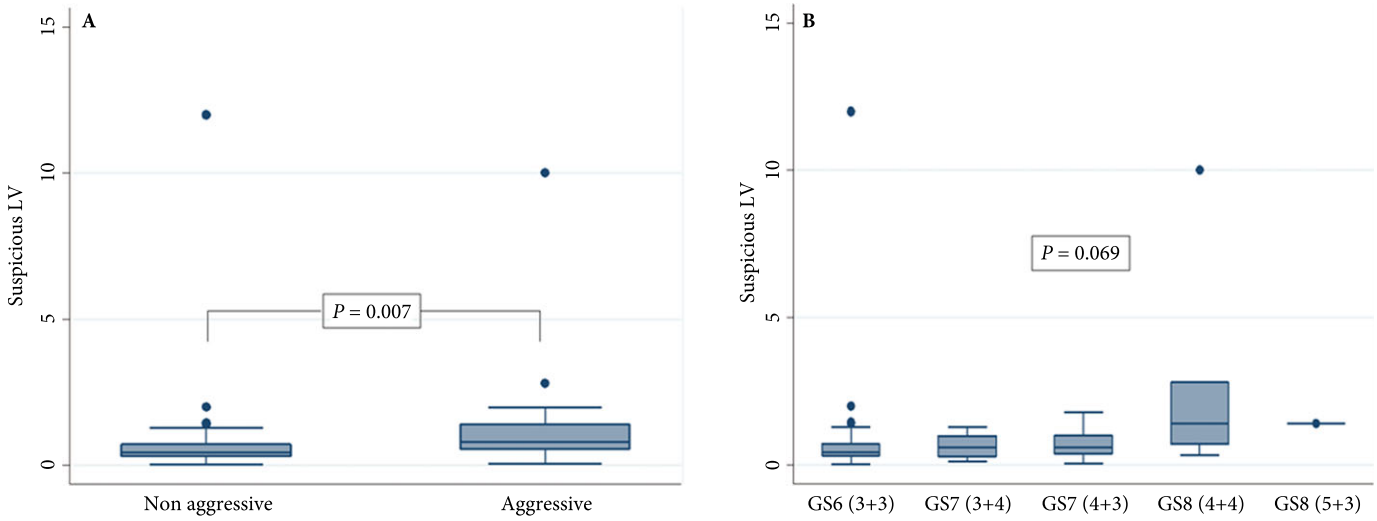

Table 5 PiGle table showing the relationship between PI-RADS score and biopsy Gleason score.

PI-RADS v2 score	Positive, *n*					Total, *n*	*P*
	Gleason score 6 (3 + 3)	Gleason score 7 (3 + 4)	Gleason score 7 (4 + 3)	Gleason score 8 (4 + 4)	Gleason score 8 (5 + 3)		
1	0	0	0	0	0	0	0.03
2	3	0	0	0	0	3	
3	8	1	0	0	0	9	
4	27	5	2	3	1	38	
5	11	5	3	4	1	24	
Total, *n*	49	11	5	7	2	74	

Tumour aggressiveness increased with increasing PI-RADS score.

Table 6 PiVoGle table showing the relationship between PI-RADS score, LV and Gleason score.

PI-RADS v2	*N*	LV, mL	Positive Gleason score, *n*					Subtotal, *n* total	Negative, *n*	Total, *n*
			6 (3 + 3)	7 (3 + 4)	7 (4 + 3)	8 (4 + 4)	8 (5 + 3)			
1	6	≤0.5	0	0	0	0	0	0	6	6
		0.5–1	0	0	0	0	0	0	0	0
		≥1	0	0	0	0	0	0	0	0
2	108	≤0.5	3	0	0	0	0	3	74	77
		0.5–1	0	0	0	0	0	0	22	22
		≥1	0	0	0	0	0	0	9	9
3	75	≤0.5	5	0	0	0	0	5	43	48
		0.5–1	1	0	0	0	0	1	12	13
		≥1	2	1	0	0	0	3	11	14
4	66	≤0.5	14	1	2	0	0	17	15	32
		0.5–1	10	3	0	2	0	15	11	26
		≥1	3	1	0	1	1	6	2	8
5	28	≤0.5	3	1	0	0	0	4	1	5
		0.5–1	4	3	1	1	0	9	1	10
		≥1	4	1	2	3	1	11	2	13
Total, *n*			49	11	5	7	2	74	209	283

This table permits calculation of the prostate cancer and significant prostate cancer risk of each lesion considering its PI-RADS score and LV. For example, the prostate cancer risk of a lesion with PI-RADS score 4 and LV between 0.5 and 1 mL is 15/26 = 57.7% and its significant prostate cancer risk is 5/26 = 19.2%, and so on.

cancer detection was 0% for SLs with PI-RADS scores of 1, 2 and 3; this increased to five of 26 (19.2%) for SLs with PI-RADS scores of 4 and five of 10 for SLs with PI-RADS scores of 5 ($P < 0.001$). Finally, for the SL group with a LV of ≥1 mL, significant prostate cancer detection was 0% for SLs with PI-RADS scores of 1 and 2, one of 14 for SLs with a PI-RADS score of 3, three of eight for PI-RADS scores of 4 and seven of 13 for SLs with a PI-RADS score of 5 ($P = 0.008$).

Similar to the relationship with PI-RADS score, the significant prostate cancer detection rate proportionally increased with the increasing LV when considering the same PI-RADS score, although statistical significance was not achieved with our data. For example, considering the PI-RADS score 4 group, the significant prostate cancer detection was three of 32 (9.4%) for a LV of ≤0.5 mL, increasing to five of 26 (19.2%) for a LV of 0.5–1 mL, and three of eight for a LV of ≥1 mL ($P = 0.1$).

There were no severe postoperative complications: 3.2% of patients reported moderate haematuria, 5.7% had acute urinary retention, 11.46% had perineal haematoma, and 86% had haemospermia. Neither fever nor urinary sepsis was reported (0%).

In all, 23/61 patients (37.7%) underwent RALP. The risk of having a locally extended (pT2c) or advanced (≥ pT3a) prostate cancer became statistically significant for MRI LVs of >0.5 mL ($P = 0.025$ and $P = 0.045$, respectively; Table 7).

Finally, a direct comparison between pathological and radiological findings was done. The mean (range) index MRI LV was 0.94 (0.12–3.8) mL and the index HTV was 1.13 (0.12–4.4) mL. Three index tumours (13%) incidentally detected by systematic biopsy were invisible on MRI and the mean volume for these tumours was <0.3 mL. The remaining 20 index tumours (87%) were visible on MRI. The correspondence between mpMRI findings and pathological locations of the tumour was 100%. There was a positive correlation between MRI LV and HTV ($r = 0.9876$, $P < 0.001$). Bland–Altman analysis revealed a clinically significant

Table 7 Relationship between LV and final pathological specimen.

Stage and grade after RALP	Biopsy Gleason score	LV, mL	P
pT2a Gleason score (3 + 3)	6 (3 + 3)	<0.5	Extended prostate
	6 (3 + 3)	<0.5	cancer = 0.025
	6 (3 + 3)	<0.5	Advanced prostate
pT2c Gleason score 6 (3 + 3)	6 (3 + 3)	0.5–1	cancer = 0.045
	6 (3 + 3)	0.5–1	
	6 (3 + 3)	<0.5	
	6 (3 + 3)	0.5–1	
	6 (3 + 3)	<0.5	
	6 (3 + 3)	<0.5	
pT2c Gleason score (3 + 4)	6 (3 + 3)	0.5–1	
	7 (3 + 4)	0.5–1	
pT2c Gleason score (4 + 3)	7 (4 + 3)	>1	
	7 (4 + 3)	<0.5	
pT3a Gleason score 6 (3 + 3)	6 (3 + 3)	<0.5	
	6 (3 + 3)	>1	
	6 (3 + 3)	>1	
pT3a Gleason score7 (3 + 4)	6 (3 + 3)	<0.5	
pT3a Gleason score 7(4 + 3)	7 (3 + 4)	0.5–1	
	7 (4 + 3)	>1	
pT3a Gleason score 8 (3 + 5)	8 (5 + 3)	>1	
pT3b Gleason score 6 (3 + 3)	6 (3 + 3)	0.5–1	
pT3b Gleason score 7 (4 + 3)	8 (4 + 4)	>1	
pT3b Gleason score 9 (4 + 5), N1	8 (4 + 4)	>1	

A LV of >0.5 mL is significantly associated both with local extended and with local advanced prostate cancer when compared with final specimens.

bias in the agreement between MRI LV and HTV. MRI LV was underestimated by 4.2% (95% CI 2–8.2%) compared to HTV (Fig. 8).

Discussion

mpMRI is an evolution of standard MRI and it has been shown that its clinical application helps to manage suspected and confirmed prostate cancer [17]. mpMRI increases the clinical diagnostic yield of prostate cancer compared to US, with a proven correlation between PI-RADS score and tumour detection, while the correlation between PI-RADS score and tumour aggressiveness is still debatable [18,19]. When used to perform FTBx, mpMRI has been shown to increase diagnostic yield for significant prostate cancer compared to simple TRUS-guided biopsy [20–22].

As the volume of a cancerous lesion is increasingly incorporated into significant prostate cancer definitions, a crucial issue is the correct estimation of TV by mpMRI [23]. In fact, the evaluation of LV before biopsy should add important information for understanding the risk of the lesion itself, to identify the patients in which FTBx is required and to make the correct decision if prostate cancer is diagnosed at FTBx.

Several studies have evaluated the correspondence between mpMRI LV and HTV on radical prostatectomy specimens [14,24], finding a positive correlation with an underestimation of mpMRI LV ranging from 5.9% (without shrinkage factor) to 20% (using a shrinkage factor of 1.15). In our present study, we compared MRI LV and HTV measurement without using a correction factor and the results were comparable with those obtained by Baco et al. [14].

Fig. 8 (**A**) Scatter plot showing correlation between MRI-estimated tumour volume (mpMRI LV) and histological tumour volume (HTV) in 23 patients. The red line indicates the regression line. (**B**) Bland–Altman plot showing the limitation of agreement between mpMRI LV and HTV. The orange line represents the linear regression line. The percentage difference between mpMRI LV and HTV is plotted against the average tumour volume (calculated from both mpMRI LV and HTV). All values above the zero line represent overestimation of mpMRI LV, and all values below the zero line represent underestimation of mpMRI LV. The average underestimation of HTV by MRI is 4.2% (95% CI 2–8.2%), and is constant throughout the measurement range. The limit of agreement ranges from −0.54 to +0.15, which indicates clinically significant inaccuracy for mpMRI LV. The median (range) is 0.72 (0.12–3.8) mL for mpMRI LV and 0.89 (0.12–4.4) mL for HTV. Graphic generated using MedCalc Software bvba version 16.4.3.

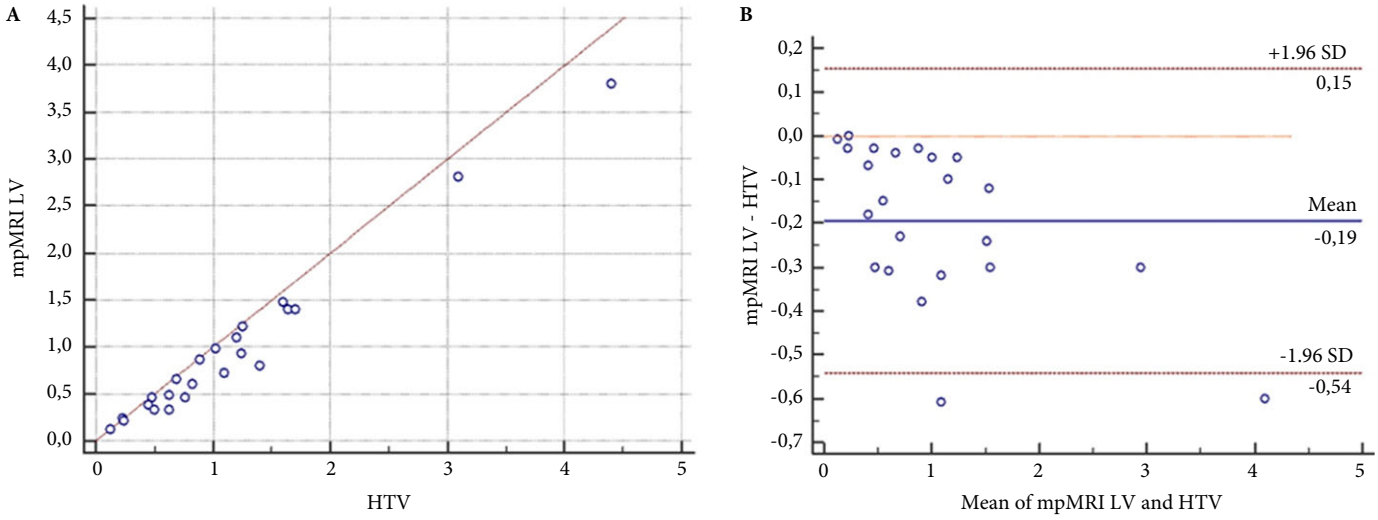

As indicated by many authors [18–20], our present study confirms that the cancer detection rate increases with increasing PI-RADS score, being statistically significantly higher for PI-RADS score ≥4 lesions. We found that the probability of a prostate cancer diagnosis increased from 5- to 50-times when switching from PI-RADS score 3 to 4 and became 222-times higher for PI-RADS 5 lesions. Similar to the PI-RADS score, the cancer detection rate independently increased with increasing LV, being statistically significantly higher for SLs of >1 mL. We found that the probability of a prostate cancer diagnosis was 2.6-times higher for a LV between 0.5 and 1 mL, which increased to 4-times higher for a LV of >1 mL. Moreover, when matching PI-RADS score and LV, we found that within each PI-RADS lesions group the probability of a diagnosis of prostate cancer increased proportionally with LV increase.

Another concern is the ability of mpMRI to predict significant prostate cancer, which is still debated by many authors [18,25–27]. Our present study showed that a significant prostate cancer diagnosis significantly increased with PI-RADS score increase (Table 5) and with LV increase (Table 4). This is a probably a reflection of tumour biology with aggressive tumours growing quickly and thus having a high probability of having a large LV at mpMRI.

PiVoGle Table 6 shows the relationship between PI-RADS score, LV, and Gleason score allowing correlation between significant prostate cancer detection and the two variables when matched. We found that as PI-RADS score increases the probability of detecting a higher Gleason score (≥7) proportionally increases with LV increase. From the data in Table 6, we can state that lesions with a PI-RADS score ≤2 should not be sampled (prostate cancer detection rate was 2.8% with a indolent diagnosis in all cases) and that patients with lesions with a PI-RADS score of 3 and MRI LV of <0.5 mL should be informed of a low prostate cancer risk (prostate cancer detection 10.42% with an indolent diagnosis in all cases). Liddell et al. [19] based on Epstein criteria concluded that PI-RADS 3 lesions should not be sampled but monitored only because these lesions are associated with a low risk of significant prostate cancer.

The results of our present study are in agreement with those of Baco et al. [14], who showed a positive correlation between MRI LV and HTV, confirming that mpMRI does not overestimate but rather underestimates the true HTV. Based on these principles we believe that MRI LV can be particularly useful in the PI-RADS score 3 SL group for discerning whether a biopsy should be taken, including MRI LV as one of the significant prostate cancer criteria, we found that 14.8% of patients with PI-RADS score 3 and LVs >0.5 mL had significant prostate cancer. So, in our opinion MRI LV can aid clinicians in the decision of whether a SL should undergo FTBx.

Finally, Wolters et al. [27] reported a positive relationship between a LV of >0.5 mL at radical prostatectomy, prostate cancer staging and Gleason score. Similarly, although our RALP series was small, we found that mpMRI LV was independently correlated with tumour local extension and a LV of >0.5 mL was significantly associated both with local extended and local advanced prostate cancer.

The limits of the present study include its retrospective design. Moreover, data are related to a single centre and to a limited cohort and therefore cannot be considered conclusive. These findings should be investigated in a multicentre study in a larger cohort of patients to validate and assess the definitive prostate cancer risk for each LV group. Finally, no shrinkage factor was used to normalise the underestimation of mpMRI LV. Nevertheless, clinical application of our tables should help urologists to determinate prostate cancer risk of each patient based on mpMRI SL characteristics.

Conclusion

Our experience with FTBx has shown substantial advantages for overall prostate cancer detection and an increase in significant prostate cancer detection. The present study shows that PI-RADS score and LV, independently and matched, are associated with prostate cancer detection and with tumour clinical significance.

Acknowledgments

We thank Mr Jonathan Brereton Jones from Linguistic centre of the University of Modena and Reggio Emilia for his help in the article English revision.

Conflicts of Interest

None.

References

1 **Fütterer JJ, Briganti A, De Visschere P et al.** Can clinically significant prostate cancer be detected with multiparametric magnetic resonance imaging? A systematic review of the literature. *Eur Urol* 2015; 68: 1045–53

2 **Hoeks CM, Barentsz JO, Hambrock T et al.** Prostate cancer: multiparametric MR imaging for detection, localization, and staging. *Radiology* 2011; 261: 46–66

3 **Delongchamps NB, Beuvon F, Eiss D et al.** Multiparametric MRI is helpful to predict tumor focality, stage, and size in patients diagnosed with unilateral low-risk prostate cancer. *Prostate Cancer Prostatic Dis* 2011; 14: 232–7

4 **Delongchamps NB, Rouanne M, Flam T et al.** Multiparametric magnetic resonance imaging for the detection and localization of prostate cancer: combination of T2-weighted, dynamic contrast-enhanced and diffusion-weighted imaging. *BJU Int* 2011; 107: 1411–18

5 **Hamoen EH, De Rooij M, Witjes JA, Barentsz JO, Rovers MM.** Use of the Prostate Imaging Reporting and Data System (PI-RADS) for prostate cancer detection with multiparametric magnetic resonance imaging: a diagnostic meta-analysis. *Eur Urol* 2015; 67: 1112–21

6 **Weinreb JC**, **Barentsz JO**, **Choyke PL et al.** PI-RADS prostate imaging - reporting and data system: 2015, Version 2. *Eur Urol* 2016; 69: 16–40

7 **Schoots IG**, **Roobol MJ**, **Nieboer D**, **Bangma CH**, **Steyerberg EW**, **Hunink MG**. Magnetic resonance imaging-targeted biopsy may enhance the diagnostic accuracy of significant prostate cancer detection compared to standard transrectal ultrasound-guided biopsy: a systematic review and meta-analysis. *Eur Urol* 2015; 68: 438–50

8 **Barentsz JO**, **Weinreb JC**, **Verma S et al.** Synopsis of the PI-RADS v2 guidelines for multiparametric prostate magnetic resonance imaging and recommendations for use. *Eur Urol* 2016; 69: 41–9

9 **Hansen N**, **Patruno G**, **Wadhwa K et al.** Magnetic resonance and ultrasound image fusion supported transperineal prostate biopsy using the Ginsburg protocol: technique, learning points, and biopsy results. *Eur Urol* 2016; 70: 332–40

10 **Moore CM**, **Kasivisvanathan V**, **Eggener S et al.** Standards of reporting for MRI-targeted biopsy studies (START) of the prostate: recommendations from an International Working Group. *Eur Urol* 2013; 64: 544–52

11 **Matyka M**, **Ollila MA**. Pressure model for soft body simulation. Conference Proceedings from SIGRAD2003. Available at: http://www.ep.liu.se/ecp/010/007/ecp01007.pdf. Accessed September 2016

12 **Ancona MG**. *Computational Methods for Applied Science and Engineering: An Interactive Approach*, Paramus, NJ, USA: Rinton Press, 2002

13 **Matyka M**. How To Implement a Pressure Soft Body Model, March 30, 2004. Available at: maq@panoramix.ift.uni.wroc. Accessed September 2016.

14 **Baco E**, **Ukimura O**, **Rud E et al.** Magnetic resonance imaging-transectal ultrasound image-fusion biopsies accurately characterize the index tumor: correlation with step-sectioned radical prostatectomy specimens in 135 patients. *Eur Urol* 2015; 67: 787–94

15 **Perera M**, **Lawrentschuk N**, **Bolton D**, **Clouston D**. Comparison of contemporary methods for estimating prostate tumour volume in pathological specimens. *BJU Int* 2014; 113(Suppl. 2): 29–34

16 **Kuru TH**, **Wadhwa K**, **Chang RT et al.** Definitions of terms, processes and a minimum dataset for transperineal prostate biopsies: a standardization approach of the Ginsburg Study Group for Enhanced Prostate Diagnostics. *BJU Int* 2013; 112: 568–77

17 **Le JD**, **Tan N**, **Shkolyar E et al.** Multifocality and prostate cancer detection by multiparametric magnetic resonance imaging: correlation with whole-mount histopathology. *Eur Urol* 2015; 67: 569–76

18 **Cash H**, **Maxeiner A**, **Stephan C et al.** The detection of significant prostate cancer is correlated with the Prostate Imaging Reporting and Data System (PI-RADS) in MRI/transrectal ultrasound fusion biopsy. *World J Urol* 2016; 34: 525–32

19 **Liddell H**, **Jyoti R**, **Haxhimolla HZ**. mp-MRI prostate characterised PIRADS 3 lesions are associated with a low risk of clinically significant prostate cancer- a retrospective review of 92 biopsed PIRADS 3 lesions. *Curr Urol* 2015; 8: 96–100

20 **Valerio M**, **Donaldson I**, **Emberton M et al.** Detection of clinically significant prostate cancer using magnetic resonance imaging-ultrasound fusion targeted biopsy: a systematic review. *Eur Urol* 2015; 68: 8–19

21 **Siddiqui MM**, **Rais-Bahrami S**, **Truong H et al.** Magnetic resonance imaging/ultrasound-fusion biopsy significantly upgrades prostate cancer versus systematic 12-core transrectal ultrasound biopsy. *Eur Urol* 2013; 64: 713–19

22 **Martorana E**, **Micali S**, **Ghaith A et al.** Advantages of single-puncture transperineal saturation biopsy of prostate: analysis of outcomes in 125 patients using our scheme. *Int Urol Nephrol* 2015; 47: 735–41

23 **Wolters T**, **Roobol MJ**, **van Leeuwen PJ et al.** A critical analysis of the tumor volume threshold for clinically insignificant prostate cancer using a data set of a randomized screening trial. *J Urol* 2011; 185: 121–5

24 **Radtke JP**, **Schwab C**, **Wolf MB et al.** Multiparametric magnetic resonance imaging (MRI) and MRI-transrectal ultrasound fusion biopsy for index tumor detection: correlation with radical prostatectomy specimen. *Eur Urol* 2016; [Epub ahead of print]. doi: 10.1016/j.eururo.2015.12.052

25 **Litjens GJ**, **Barentsz JO**, **Karssemeijer N**, **Huisman HJ**. Clinical evaluation of a computer-aided diagnosis system for determining cancer aggressiveness in prostate MRI. *Eur Radiol* 2015; 25: 3187–99

26 **Dwivedi DK**, **Kumar R**, **Bora GS et al.** Stratification of the aggressiveness of prostate cancer using pre-biopsy multiparametric MRI (mpMRI). *NMR Biomed* 2016; 29: 232–8

27 **Wolters T**, **Roobol MJ**, **van Leeuwen PJ et al.** Should pathologists routinely report prostate tumour volume? The prognostic value of tumour volume in prostate cancer. *Eur Urol* 2010; 57: 821–9

Correspondence: Eugenio Martorana, Department of Urology, Policlinico di Modena, Via del Pozzo, 71 Modena 41124, Italy.

e-mail: eugeniomartorana@libero.it

Abbreviations: ADC, apparent diffusion coefficient; ASAP, atypical small acinar proliferation; DCE, dynamic contrast-enhanced; 3D, three-dimensional; DWI, diffusion-weighted imaging; FSE, fast spin-echo; FTBx, transperineal prostate US/MRI fusion-targeted biopsy; HGPIN, high-grade prostatic intraepithelial neoplasia; HTV, histological tumour volume; LV, lesion volume; mpMRI, multiparametric MRI; PI-RADS, Prostate Imaging Reporting and Data System; RALP, robot-assisted laparoscopic radical prostatectomy; ROI, region of interest; SL, suspicious lesion; START, Standards of reporting for MRI-targeted biopsy studies; T2W, T2-weighted; US, ultrasonography; VOI, volume of interest.

